PNAS
www.pnas.org

Supplementary Information for

Maturation of polycistronic mRNAs by the endoribonuclease RNase Y and its associated Y-complex in *Bacillus subtilis*

Aaron DeLoughery[1], Jean-Benoît Lalanne[1,2], Richard Losick[3], Gene-Wei Li[1*]

[1]Department of Biology, Massachusetts Institute of Technology, Cambridge, MA, USA
[2]Department of Physics, Massachusetts Institute of Technology, Cambridge, MA, USA
[3]Department of Molecular and Cellular Biology, Harvard University, Cambridge, MA, USA

Gene-Wei Li
Email: gwli@mit.edu

This PDF file includes:

Supplementary text with extended methods
Figs. S1 to S6
Captions for Datasets S1 to S4
References for SI reference citations

Other supplementary materials for this manuscript include the following:

Datasets S1 to S4

www.pnas.org/cgi/doi/10.1073/pnas.1803283115

Supplementary Information Text

Extended Materials and Methods

Bacterial strains and media:

Unless otherwise noted, *Bacillus subtilis* strains 3610, PY79, 168, and their derivatives were grown in Luria-Bertani (LB) medium (10 g tryptone, 5 g yeast extract, and 5 g NaCl per liter) in liquid shaking culture or on agar plates (1.5% Bacto-agar) at 37°C. *S. aureus* was grown in tryptic soy broth (TSB; EMD Millipore) and on LB agar. When necessary, antibiotics were added to the media, for *B. subtilis* strains: spectinomycin (100 μg/ml), kanamycin (10 μg/ml), chloramphenicol (5 μg/ml), and mls (erythromycin 0.5 μg/ml and lincomycin 2.5 μg/ml), for *E. coli*: ampicillin (100 μg/ml), and for *S. aureus* tetracycline (3 μg/ml) or chloramphenicol (10 μg/ml). MSgg media is composed of 5 mM potassium phosphate (pH7.0), 100 mM MOPS (pH 7.0), 2 mM $MgCl_2$, 700 μM $CaCl_2$, 50 μM $MnCl_2$, 50 μM $FeCl_3$, 1 μM $ZnCl_2$, 2 μM thiamine, 0.5% glycerol, 0.5% glutamic acid, 50 μg/ml tryptophan, 50 μg/ml threonine, and 50 μg/ml phenylalanine. Biofilms were grown on LB glycerol manganese 1.5% agar (LB, 1% glycerol, 10 mM $MnCl_2$) (1) at room temperature for 5 days and imaged on a gel imaging doc (BioRad, Carlsbad, CA).

For Rend-seq experiments, *B. subtilis* 3610 with a deletion of *epsH* was used as wild type. This deletion prevents matrix production. The *epsH* deletion does not affect the Y-complex and RNase Y dependent isoforms as these isoforms are present in other wild type samples with an intact *eps* operon, such as *B. subtilis* 168 (8).

Strain construction:

Antibiotic marked fragments of DNA were introduced into PY79 or 168 by transformation (2, 3) and into 3610 by SPP1 phage transduction (3). Insertional deletions of *rny* and *pnpA* were created as described (4). The markerless YaaT-GFP fusion was created using pminimad2 (5). Construction of unmarked *ylbF* deletion in HG003 was performed as previously described (6) using pKFC or pKFT vectors (7). Isothermal assembly products were transformed in *E. coli* DC10B. Plasmids were transformed directly into HG003 with selection on tetracycline (for pKFT) or chloramphenicol (for pKFC) at 30°C. See Dataset S4 for deletion construct details and for primer sequences.

Growth for RNA sequencing and RNA extraction

For all samples, overnight cultures were back diluted to an OD_{600} of 0.001 in 25 ml of LB or MSgg. Cells from exponential cultures were collected at OD_{600} of 0.25 –0.3. Stationary phase cells from MSgg were collected at an OD_{600} of ≈2.5. *S. aureu*s was grown in TSB and cells were collected at an OD_{600} of ≈0.5. At the indicated point, 10 ml of each culture was mixed with 10 ml of ice cold methanol and spun down at 3220 ×g at 4 °C for 10 minutes. Supernatant was discarded and cell pellets were frozen in liquid nitrogen and stored at -80°C. For RNA extraction, the thawed pellets were resuspended in 1 ml of Trizol reagent (Thermo Fisher, Waltham, MA) and added to FastPrep lysis matrix

B 2 ml tubes with beads (MP Biomedicals). Cells were disrupted in a Bead Ruptor 24 (Omni International, Kennesaw, GA) twice for 40 seconds at 6.0 M/s. 200 µl of chloroform was and were kept at room temperature for 2 minutes after vigorous vortexing. Mixture was spun down at 18,200 ×g for 30 minutes at 4 °C. The aqueous phase (~600 µl) was precipitated with 900 µl of isopropanol for 10 minutes at room temperature. The RNA pellet was collected and washed with 80% ethonal, and resuspended in 200 µl 10 mM Tris-HCl pH 7.0. Approximately 50 µg of RNA was applied to a Qiagen RNeasy column and treated with DNase according to the manufacturers (Qiagen, Hilden, Germany).

Rend-seq library preparation.
Throughout, RNA was precipitated with 50% isopropanol, 150 mM sodium acetate pH 5.5, and 30 µg of GlycoBlue Coprecipitant (ThermoFisher) and DNA with 50% isopropanol, 32 µl of 5M NaCl, 1 µl of 0.5 M EDTA, and 30 µg of glycogen blue for 30 min at -80°C. Precipitated nucleic acids were centrifuged at 18,200 ×g for 30 minutes at 4°C. The pellet was washed with 500 µl of cold 80% ethanol. The ethanol was removed and the pellet was dried at room temperature for 10 minutes. RNA was resuspended in 10 mM Tris-HCl ph 7.0 and DNA was resuspended in 10 mM Tris-HCl pH 8.0. For denaturing polyacrylamide gel electrophoresis were prepared using Novex-TBE-Urea sample buffer (ThermoFisher) and denatured for 2 min. at 80°C. SYBR gold nucleic acid stain was used to image and excise nucleic acids (ThermoFisher).

For the sequencing library, total DNase treated RNA (5-10 µg) was depleted of rRNA using MICROBExpress (ThermoFisher) using 8 µl of capture oligo instead of 4 µl. RNA depleted of rRNA was precipitated and resuspended into 40 µL of 10 mM Tris HCl. The RNA was fragmented by first heating the sample to 95°C for 2 min and adding RNA fragmentation buffer (1x, Thermo Fisher) for 30 seconds at 95°C and quenched by addition of RNA fragmentation stop buffer (ThermoFisher). Samples were precipitated and fragmented RNAs between 20 and 40 bp were isolated by size excision from a denaturing polyacrylamide gel (15%, TBE-Urea, 65 min., 200 V, ThermoFisher). Size selected fragments were dephosphorylated using T4 polynucleotide kinase (New England Biolabs, Ipswitch, MA), precipitated, and ligated to 5' adenylated and 3'-end blocked linker 1 (IDT 5 µM) using T4 RNA ligase 2, truncated K227Q. The ligation was carried out at 25°C for 2.5 hours using <5 pmol of dephosphorylated RNA in the presence of 25% PEG 8000 (ThermoFisher) and heat inactivated for 10 min at 80°C. Ligation products from 35 to 65 bp were excised after denaturing PAGE (10% TBE-Urea, 50 min., 200 V, ThermoFisher). cDNA was prepared by reverse transcription of ligated RNA using Superscript III (ThermoFisher) at 50°C for 30 min. with primer oCJ485 (sequence in Dataset S4, IDT, Coralville, Iowa) and the RNA was hydrolyzed with the addition of 2.3 µl of 1 M NaOH and incubated at 95 °C for 15 minutes. cDNA was isolated by PAGE size excision (10% TBE-Urea, 200V, 80 min., ThermoFisher). Single stranded cDNAs were circularized using CircLigase (Illumina, San Diego, CA) at 60°C for 2 hours, 1 µl of enzyme added at the start and an additional 1 µl of enzyme after 1 hour. Circularized cDNA was the template for PCR amplification using Phusion DNA polymerase (New England Biolabs) with Illumina sequencing primers, primer o231 (IDT) and barcoded indexing primers (IDT). After 6 – 10 rounds of PCR amplification, the product was

selected by size from a non-denaturing PAGE (8% TB, 45 min., 180V, Life Technologies). For dataset names and barcode information see Dataset S4.

Exonuclease treatment
Total RNA from *B. subtilis* strain 168 exponential growth in LB were depleted of rRNA (10 µg) and treated with 5' monophosphate specific exonuclease (Illumina) for 1 hour at 30°C in the kit's buffer A. Treated samples were precipitated and incorporated into sequencing library prep at the fragmentation step.

RNA-sequencing and data analysis.
Sequencing was performed on an Illumina HiSeq 2000. The 3' linker sequences were stripped. Bowtie v. 1.2.1.1 (options -v 1 -k 1) was used for sequence alignment to the reference genome NC 000964.3 (*B. subtilis* chromosome), KF365913.1 (*B. subtilis* plasmid pBS32) and NC 007795.1 (*S. aureus*) obtained from NCBI Reference Sequence Bank. To deal with non-template addition during reverse transcription, reads with a mismatch at their 5' end had their 5' end re-assigned to the immediate next downstream position. The 5' and 3' ends of mapped reads between 15 and 45 nt in sizes were counted separately at genomic positions to produce wig files. The wig files were normalized per million non-rRNA and non-tRNA reads for each sample. Shadows were removed from wig files first by identifying the position of peaks and then by reducing the other end of the aligned reads by the peak's enrichment factor to produce the final normalized and shadow removed wig files (8). Gene regions were plotted in MATlab. A table of specific positions for each gene (Dataset S4). To compare gene levels, we take steady-state mRNA abundances for a gene of interest to be proportional to the mean read density (equal to the mean read counts) mapping to that gene. Specifically, for a gene with starting position x_{start} and end position x_{end} (nucleotide position along the genome), the read counts of the 3' ends of reads aligning to the strand of the gene at each position between $x_{start} + G$ and $x_{end} - G$ are stored. A gap G of 50 nt is chosen to avoid aberrant read counts from any remaining peak shadows. For riboswitch quantification, a gap of 10 nt was taken due to their short sizes. To avoid variability arising from PCR overamplification and cloning bias, 1% winsorization is applied to the read count distribution (the top and bottom 1% read counts are respectively replaced by the 1st and 99th read count percentile in the region). The mean read density for the gene is then taken as the mean of the winsorized read count distribution.

Systematic identification of mRNA isoform maturation by RNase Y
To identify maturation events by RNase Y throughout the transcriptome, we used an automated mRNA end finding strategy for Rend-seq data described in Lalanne et al, 2018 (8) with the following modifications.

The peak z score (z score of read counts at position x, excluding a window of 5 nucleotide centered at x, averaging over a region 100 nt wide) was computed at all genomic positions in WT (from the published data in strain 168) (8) and Δ*rny* Rend-seq data. To reduce the number of false positives arising from slight shift in peak positions (arising from technical variability), the peak z score at each position x was replaced by the maximum z score in region from x-2 to x+2 nt.

Processing events by RNase Y are indicated by 5'-ends of transcripts in WT disappearing in Δ*rny*. We thus identified positions with peak z>13.5 in WT and z<3.5 in Δ*rny*, leading to roughly one hundred candidate positions. The candidates were subsequently manually curated to identify the subset that corresponded to *bona fide* processing/maturation events that lead to truncated isoforms from the 5' end (i.e. disappearance of truncated isoforms in the 5' exonuclease treated Rend-seq data) and to assess Y-complex dependence of the cleavage. In addition, peaks were assessed for a step in read density between upstream and downstream regions in the wild type data, as would be expected for a maturation event that leads to an unstable 5' fragment. We reported high-confidence processing sites whose downstream level is at least 20% higher than the upstream level. We also require that the read density downstream of the processed 5' end is greater than 0.5 reads per nucleotide. Dataset S1 lists the 22 high-confidence candidates for RNase Y mediated processing. In addition to these examples, there are two other likely examples of a RNase Y cleavage events in the genes *dps* and *tagD*, which we were unable to calculate a step in read density due to their proximity other peaks or transcription start sites.

We likely underestimated the number of processing events because not every operon is expressed under the conditions used in this study. We also cannot exclude missed processing events (false negative) from the selected peak z score threshold. In addition, the automated pipeline is not well suited to identify cleavage sites nearby other ends of transcripts, such as *dps*, as the z score for peaks is artificially reduced due to the neighboring peaks. By scanning throughout the data, we fortuitously identified such 5' UTR processing events in *menA* and *tagA* with cleavages very close to the putative TSS. We cannot exclude that other such sites are missed by our automated peak finding strategy. The list in Data S1 therefore is a conservative report for the number of operon mRNAs matured by RNase Y.

Fluorescence microscopy

Micrographs of YaaT-GFP in the wild type and Δ*ylbF* backgrounds were acquired on an Olympus BX61 upright fluorescence microscope with a 100X objective (Olympus, Tokyo, Japan). Cells were immobilized on 2.5% agarose pads. Micrographs of YaaT-GFP in the Δ*rny* background were acquired on a Nikon Ti-E inverted microscope and a CoolSnap HQ camera (Nikon, Tokyo, Japan)(Photometrics, Tucson, AZ). Nikon Intensilight mercury illuminator and chroma filter 49002 were used to create fluorescent images. Images were processed using image J fiji. Cells were collected from exponential growth in LB, OD_{600} of ≈0.4. Cells were collected (1 ml of culture) washed in 1 X PBS then resuspended in 50 µl of PBS.

Flotation and western blot

For YaaT-GFP strains in a wild type background and lacking RNase Y, 5 ml of exponential culture were collected at an OD_{600} of ≈0.5. Cells were disrupted using a a FastPrep (MP biomedical sciences, Santa Ana, CA) in lysis buffer (10 mM Tris pH 7.5, 100 mM NaCl, 2 mM DTT, and protease inhibitor (Roche, Basel, Switzerland). 350 µl of cleared lysate was added to 100 µl of 52.5% OptiPrep density gradient medium (Sigma, St. Louis, MO) into a polycarbonate centrifuge tubes (Beckman, Brea, CA, product number 343778). 750 µl of 40% OptiPrep was layered on top followed by 800 µl of lysis

buffer. Samples were spun at 50,000 rpm (213,600 x g Beckman rotor TLS-55) in Optima Max-XP Ultracentrifuge (Beckman) for 3 hours. Fractions were collected from the top of the gradient (1-750 µl, 2-450 µl, 3-650 µl, and 4-450 µl) and protein was precipitated with 20 % TCA. For western blots, cleared whole cell lysates were run on 12.5% SDS-PAGE nupage gels (ThermoFisher) and transferred to a nitrocellulose membrane (GE Water and Process Technologies, now Suez, Paramus, NJ) by electro blotting (ThermoFisher). Rabbit anti-SigA polyclonal antibodies were used at a concentration of 1:40,000 in 5% milk TTBS. Rabbit anti-GFP polyclonal, affinity purified antibodies were used at a concentration of 1:3,000 in 3% BSA (ThermoFisher). They were visualized with goat anti-rabbit antibodies conjugated to Horseradish Peroxidase at a concentration of 1:10,000 (ThermoFisher) and were developed with Hyglow quick spray (Denville Scientific, Holliston, MA) chemiluminescent substrate (ThermoFisher). Imaged with c500 gel imaging system (Azure Biosystems, Dublin, CA).

Northern blotting

Samples for Northern blot analysis were prepared from cells grown in liquid shaking cultures of LB at an OD600 of ≈0.3. Preparations of total RNA samples from *B. subtilis* were created using a Trizol extraction as previously described (9) Samples were run on 1.5% agarose gels containing 20 mM guanidine thiocyanate (10). For a loading control, rRNA was visualized by ethidium bromide staining. RNA was transferred to Hybond-N + membranes (Amersham Biosciences, Piscataway, NJ, USA) using a capillary transfer. Transcripts were detected using radiolabeled DNA probes (≈50 nt) probes against *glnR, glnA, atpI, atpB, thiC, yabA,* and *yaaT* (Dataset S4). The specific probes are detailed in the supplemental information primer table. Hybridization and signal detection were carried out according to the manufacturer's instructions overnight at 42°C (Thermo, Ultra-Hyb). As loading controls rRNA was visualized either by ethidium bromide staining with UV imaging. Radiolabeled probes were detected by phosphoimaging (phospho storage screen GE healthcare) on a Typhoon imager (Amersham).

5' RACE for rpoB.

Total RNA was purified from wild type cells grown to an OD of 0.3 in LB. RNA was harvested with trizol (as described previously, ThermoFisher) and DNase treated using RNeasy kit (Qiagen). Reverse transcription was carried out with 2.5 µg of RNA, primer rpoB_tailing, and Superscript III (ThermoFisher) for 30 minutes at 50°C. The cDNA was cleaned up using the Oligo Clean and Concentrate kit (Zymo Research). The cDNA was tailed using Terminal Transferase (Thermo) in the presence of 10 mM dCTP and 0.1 mM ddCTP. Tailed cDNA was cleaned up using the Oligo Clean and Concentrator and eluted into 30 µl. The tailed product (2 µl) was used as a templated for PCR using the primers oLH137_G11H_TdT_adaptor and rpoB_tailing for 35 cycles with an annealing temperature of 58°C. The PCR was run on 2.0% agarose gel (Denville Scientific) with Lonza GelStar Nucleic acid Stain (Fisherscientific). The two bands produced from the long and short *rpoB* isoforms were gel purified (Qiagen) and Sanger sequenced using the primer rpoB_R2 (Quintarabio).

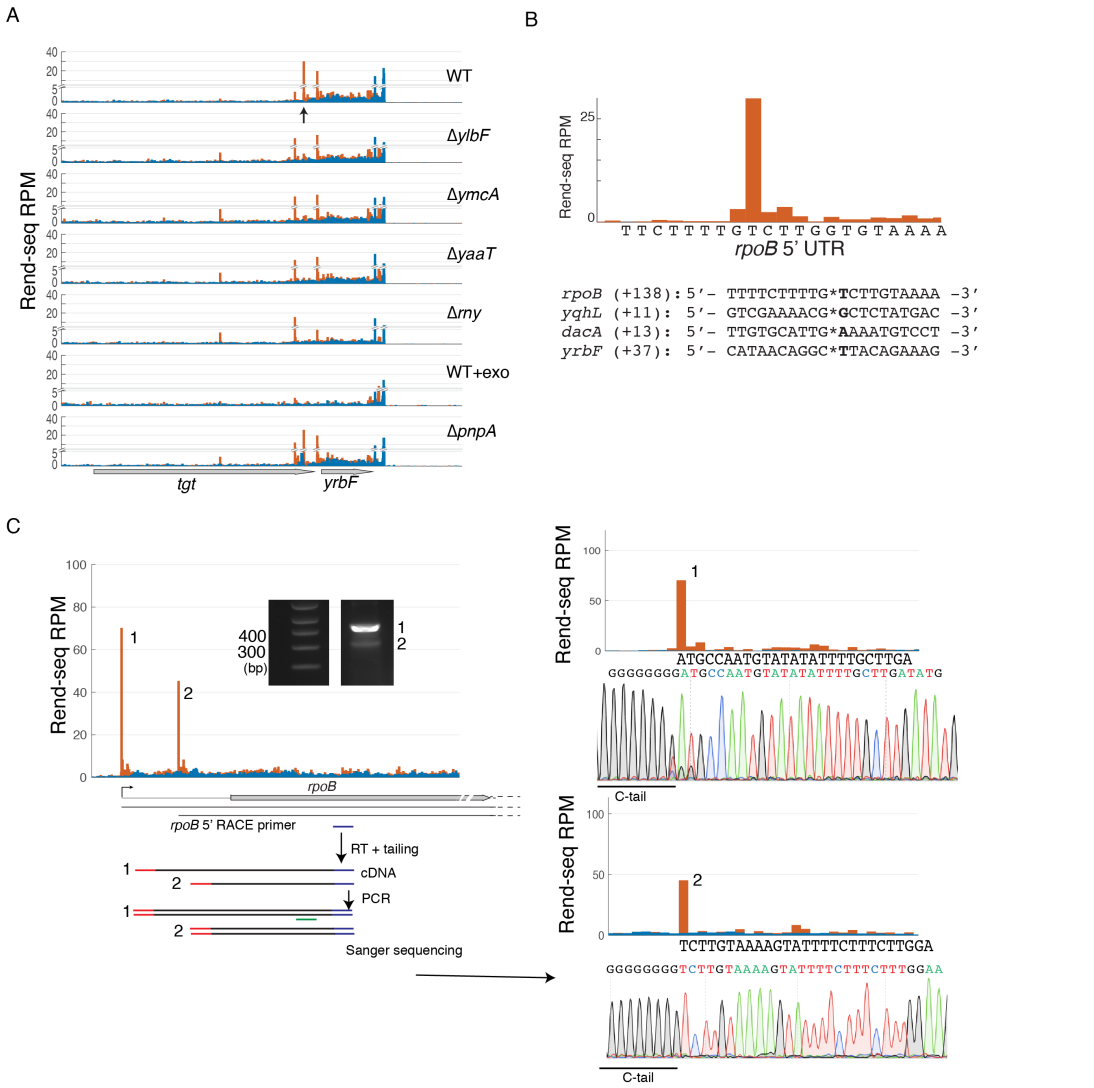

Fig. S1. Transcript isoforms of *tgt-yrbF* and confirmation of the *rpoB* UTR processing event by 5' RACE. (A) Rend-seq data showing 5'-mapped (orange) and 3'-mapped (blue) read counts plotted for the *tgt-yrbF* region of the *B. subtilis* genome from wild type cells (WT)(strain 3610, Δ*epsH* background) and mutants lacking *ylbF, ymcA, yaaT, rny*, and *pnpA* as well as wild type 5-monophosphate nuclease treated, respectively. The vertical arrow points to the position of the 5' ends of isoforms that disappear in mutants lacking components of the Y-complex. Peak shadows are removed from Rend-seq data. The Y-axis is split as indicated. **(B)** Rend-seq 5'-mapped reads surrounding 5' end of the shorter UTR isoform for the *rpoB* gene. For each example of Y-complex-dependent isoform, the position that corresponds to the 5' end is indicated in bold, and the flanking 10 nucleotides are shown. **(C)** Rend-seq data showing 5'-mapped (orange) and 3'-mapped (blue) read counts plotted for the *rpoB* region of the *B. subtilis* genome from wild type cells (WT)(strain 3610, Δ*epsH* background). A schematic of the reverse transcription, tailing, and PCR for 5' RACE is shown. The two PCR products were run on a 2.0% agarose gel. For each of the 5' ends (1 and 2) Sanger sequencing traces are shown under the Rend-seq data mapped to each peak. RPM, reads per million.

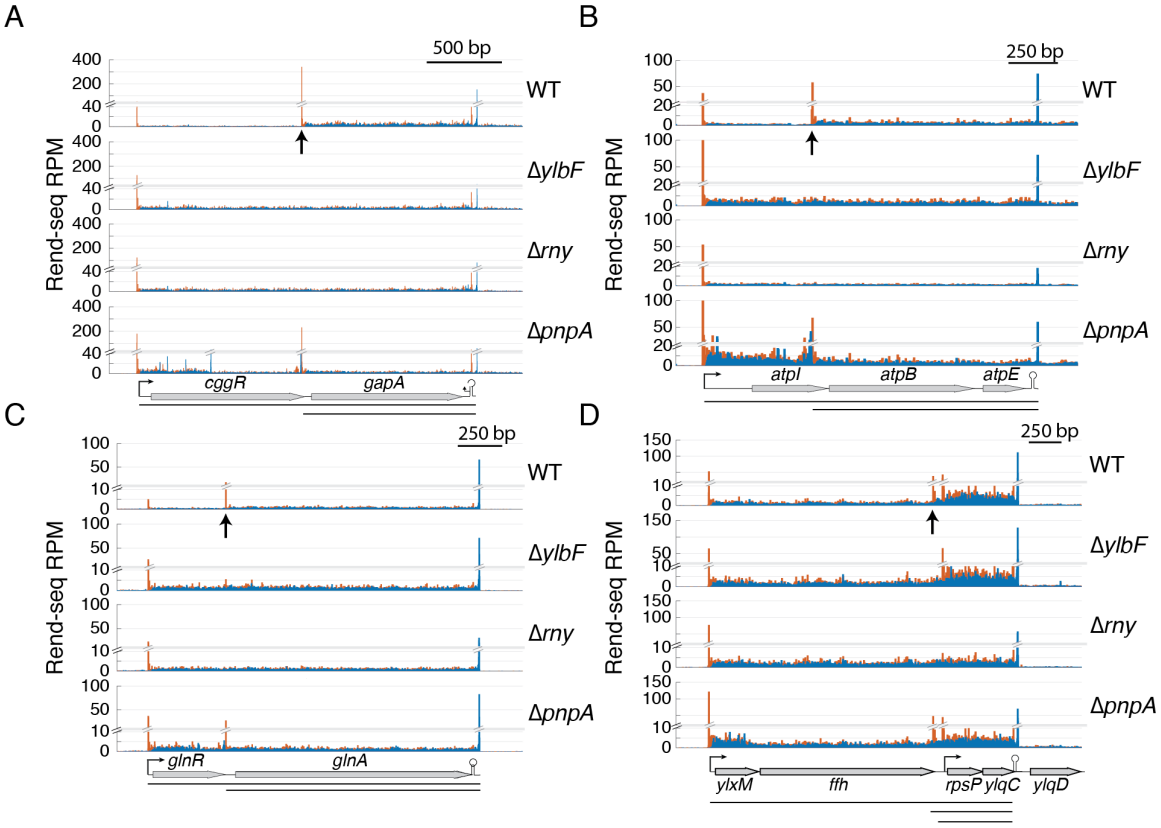

Fig. S2. Transcript isoforms in *B. subtilis* lacking the proteins YlbF, RNase Y, and PnpA. (A-D) Rend-seq data showing 5'-mapped (orange) and 3'-mapped (blue) read counts plotted for the *cggR-gapA* **(A)**, *glnR-glnA* **(B)**, *atpI-atpB-atpE* **(C)**, and *ylxM-ffh-rpsP-ylqD* **(D)** regions of the *B. subtilis* genome from wild type cells (WT)(strain 3610, Δ*epsH* background) and mutants lacking *ylbF, rny*, and *pnpA*, respectively. Horizontal lines below gene annotations indicate potential isoforms predicted by Rend-seq for wild type cells. Longer isoforms due to partial read-through of transcription terminators after *gapA*, *atpE*, and *ylqD* are not depicted. Vertical arrows point to positions of the 5' ends of isoforms that disappear in mutants lacking components of the Y-complex. Peak shadows are removed from Rend-seq data. The Y-axis is split as indicated. RPM, reads per million.

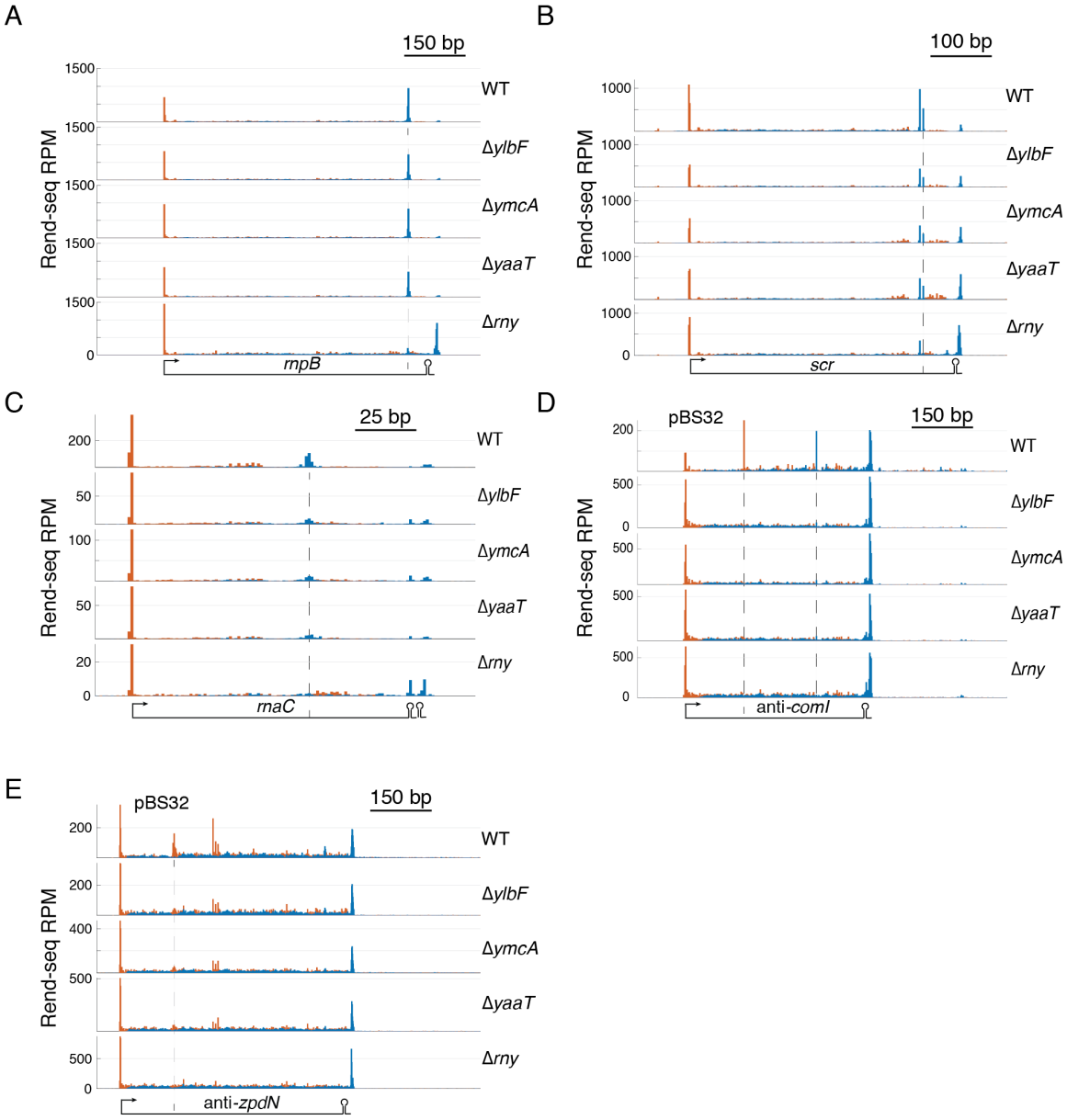

Fig. S3. Noncoding RNA maturation by RNase Y and its dependency on the Y-complex. (A-C) Rend-seq 5'-mapped (orange) and 3'-mapped (blue) read counts plotted for the *rnpB* **(A)**, *scr* **(B)**, and *rnaC* **(C)** regions of the *B. subtilis* genome from wild type cells (Δ*epsH* background) and mutants lacking *ylbF, ymcA, yaaT*, and *rny*. Dotted lines indicate the positions of mature 3' ends. **(D)** Rend-seq data from wild type cells and mutants lacking *ylbF, ymcA, yaaT, and rny* mapped to the *B. subtilis* 3610 plasmid pBS32 for the region antisense to *comI* **(E)** and antisense to *zpdN* **(F)**. Dotted lines indicate the position of RNA ends that depend on the presence of RNase Y. Peak shadows are removed from Rend-seq data. RPM, reads per million.

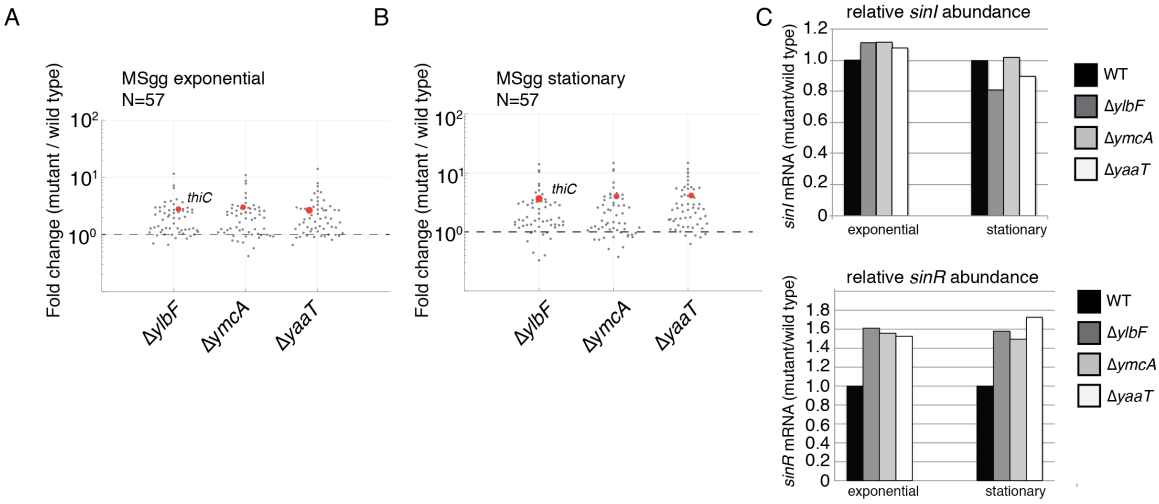

Fig. S4. Changes in riboswitch and *sinI*/*sinR* mRNA abundance in mutants lacking the Y-complex in the biofilm promoting medium MSgg. **(A-B)** The fold-change in riboswitch abundance in mutants lacking *ylbF, ymcA,* and *yaaT* compared to wild type (Δ*epsH* background) during exponential **(A)** and stationary phases **(B)**. The numbers of riboswitches whose expression levels are quantified in each condition are indicated. Red dots indicate the *thiC* riboswitch. **(C)** Quantitation of the relative mRNA density for *sinI* and *sinR* compared to wild type in mutants lacking *ylbF, ymcA, yaaT,* and *rny*. For each condition the RPKM for *sinR* and *sinI* are normalized to wild type.

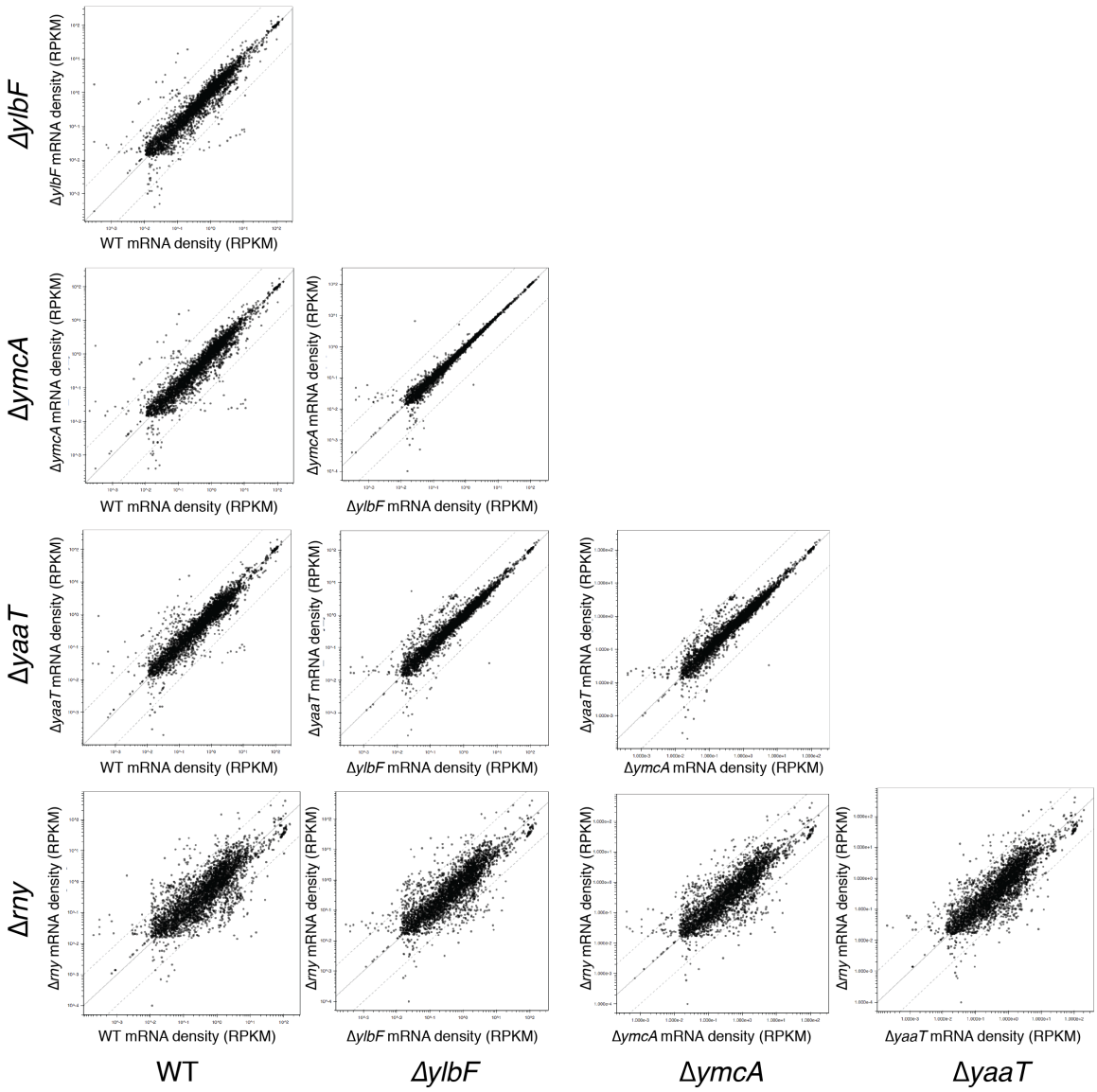

Fig. S5. Changes in mRNA abundance in wild type cells and all mutants lacking the Y-complex (A-K) mRNA abundances for all annotated and expressed genes (>50 reads) in *B. subtilis* are plotted for their levels for all combinations of wild type cells and mutants lacking *ylbF, ymcA, yaaT,* and *rny* as indicated. RNA was collected from cells in exponential phase in LB. Dashed lines indicate a 10-fold difference from the diagonal. RPKM: reads per thousand bases of gene per million bases of total reads that map to the *B. subtilis* genome, excluding rRNAs and tRNAs.

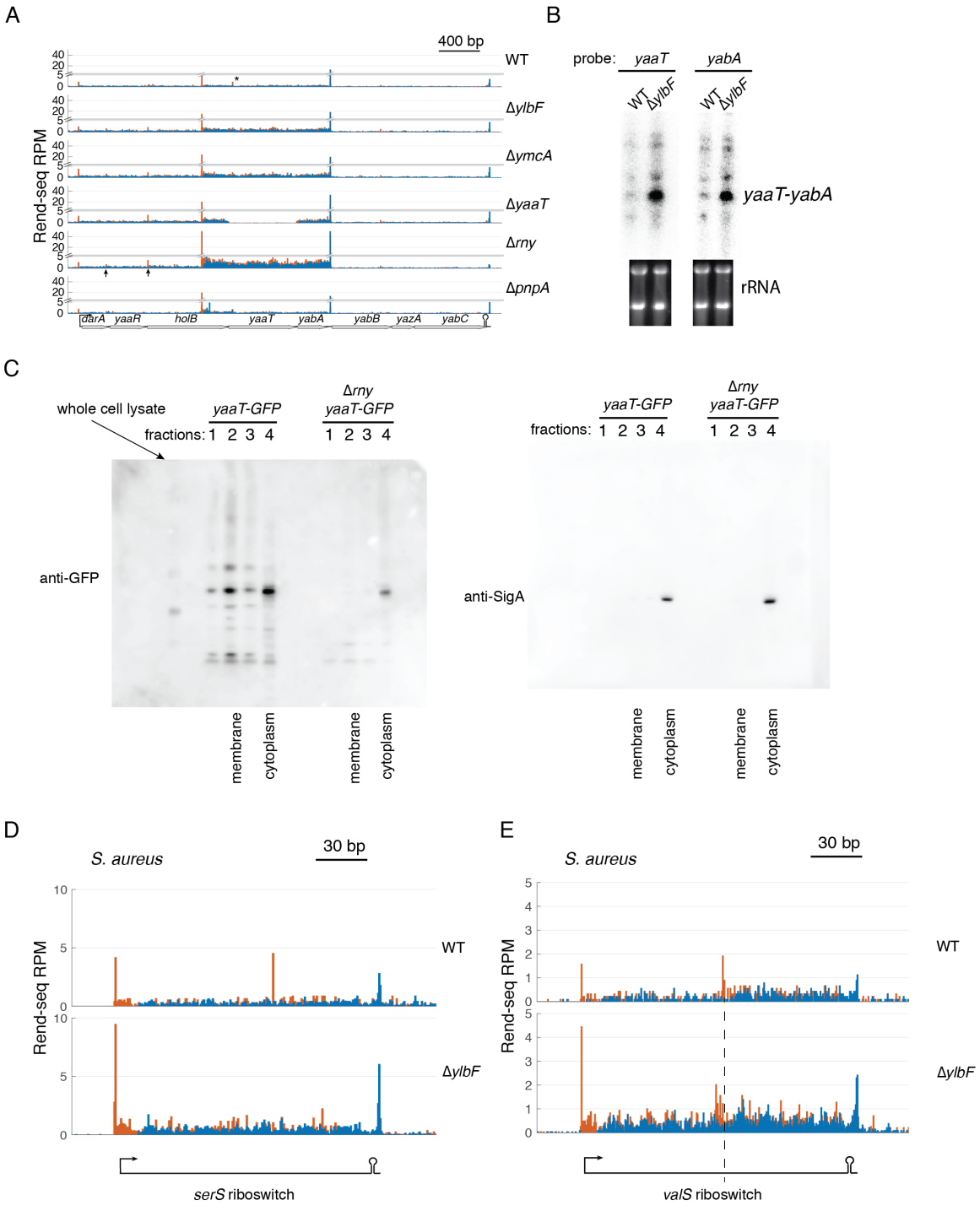

Fig. S6. Transcript isoforms of the *yaaT-yabA* region in *B. subtilis*, localization of the YaaT protein, and riboswitch processing in *S. aureus*. (A) Rend-seq 5'-mapped (orange) and 3'-mapped (blue) read counts plotted for the *yaaT* region of the genome from wild type (Δ*epsH* background) cells and cells lacking *ylbF, ymcA, yaaT, rny,* and *pnpA*. In addition to the known TSS upstream of *darA* and the TSS in *holB* reported here, small additional peaks in 5' reads of unknown origin are present and indicated with an

arrow. Peak shadows are removed from Rend-seq data. RPM, reads per million. **(B)** Northern blot analysis of the *yaaT-yabA* region of the *B. subtilis* genome in wild type cells and cells lacking *ylbF* using radiolabeled probes against *yaaT* and *yabA*. The *yabA-yaaT* transcript is identified based on size and abundance. In wild type there is a band of a smaller size that could correspond to the peak in 5' reads inside *yaaT* (indicated with an asterisk). There are also larger species that likely arise from the *darA* promoter of the other small peaks in 5' reads. Northern blots with probes to additional genes in the operon would be needed to definitively know the identity of the larger species. **(C)** Entire Western blot against YaaT-GFP (anti-GFP antibody) and SigA for fractions from a membrane flotation experiment. Cytoplasmic proteins remain in fraction 4 while membrane associated proteins migrate to fraction 2. The band shown is of the approximate size of YaaT-GFP and is absent in a wild type whole cell lysate lacking GFP. **(D)** Rend-seq 5'-mapped (orange) and 3'-mapped (blue) read counts plotted for the *serS* riboswitch of the *S. aureus* genome from wild type cells and cells lacking the ortholog of *ylbF*. **(E)** Rend-seq 5'-mapped (orange) and 3'-mapped (blue) read counts plotted for the *valS* riboswitch of the *S. aureus* genome from wild type cells and cells lacking the ortholog of *ylbF*. RPM, reads per million.

Captions for Datasets S1-S4:

Dataset S1: Operons whose maturation requires RNase Y. Operon names include all of the genes that can be in the same transcriptional unit, as evidenced by Rend-seq data. Genomic position and strand indicate the 5' end of the truncated mRNA isoform. The first complete, downstream gene of the RNase Y-dependent 5' end is indicated, as well as whether the processing leads to exclusion of upstream genes or 5' UTR. The only example of mRNA maturation by RNase Y that does not require the Y-complex is *hbs*.

Dataset S2: Levels of annotated riboswitches and leader sequences in wild type cells and mutants lacking *ymcA*, *ylbF*, and *yaaT*. Rend-seq read counts (reads per million, RPM) and read densities (reads per million per kb, RPKM) for the 65 annotated riboswitches and leader sequences are reported for the Y-complex mutants grown to exponential phase in LB, exponential phase in MSgg, or stationary phase in MSgg. For LB exponential phase, the levels in a mutant of RNase Y are also reported. The genome region and strand of each riboswitch used for calculating read counts and densities are also shown.

Dataset S3. Levels of all annotated *B. subtilis* protein-coding genes in wild type and mutants lacking *ymcA*, *ylbF*, and *yaaT*. Rend-seq read counts (reads per million, RPM) and read densities (reads per million per kb, RPKM) in Y-complex mutants grown to exponential phase in LB, exponential phase in MSgg, or stationary phase in MSgg are shown. For LB exponential phase, the mRNA abundances are also reported in a mutant of RNase Y. Of special note are increased levels in Y-complex mutants of *sinR* and *fusA* in MSgg as discussed in the Results and also of the competence inhibitor *mecA* in MSgg and LB.

Dataset S4: Strains, primers, and plasmids used in this work, the genome regions used to graph Rend-seq traces in all of the figures with the strand and bar width used, and a list of the sequencing samples with brief descriptions and barcode information.

References

1. Shemesh M & Chai Y (2013) A combination of glycerol and manganese promotes biofilm formation in Bacillus subtilis via histidine kinase KinD signaling. *Journal of bacteriology* 195(12):2747-2754.
2. Wilson GA & Bott KF (1968) Nutritional factors influencing the development of competence in the Bacillus subtilis transformation system. *Journal of bacteriology* 95(4):1439-1449.
3. Yasbin RE & Young FE (1974) Transduction in Bacillus subtilis by bacteriophage SPP1. *J Virol* 14(6):1343-1348.
4. Koo BM*, et al.* (2017) Construction and Analysis of Two Genome-Scale Deletion Libraries for Bacillus subtilis. *Cell systems* 4(3):291-305.e297.
5. Arnaud M, Chastanet A, & Debarbouille M (2004) New vector for efficient allelic replacement in naturally nontransformable, low-GC-content, gram-positive bacteria. *Appl Environ Microbiol* 70(11):6887-6891.
6. Dengler V, Foulston L, DeFrancesco AS, & Losick R (2015) An Electrostatic Net Model for the Role of Extracellular DNA in Biofilm Formation by *Staphylococcus aureus*. *J Bacteriol* 197(24):3779-3787.
7. Kato F & Sugai M (2011) A simple method of markerless gene deletion in *Staphylococcus aureus*. *Journal of Microbiological Methods* 87(1):76-81.
8. Lalanne JB, et al. (2018) Evolutionary convergence of pathway specific enzyme expression stoichiometry. Cell 173:749–761.e38.
9. Cheung AL, Eberhardt KJ, & Fischetti VA (1994) A method to isolate RNA from gram-positive bacteria and mycobacteria. *Anal Biochem* 222(2):511-514.
10. Goda SK & Minton NP (1995) A simple procedure for gel electrophoresis and northern blotting of RNA. *Nucleic acids research* 23(16):3357-3358.